Tunable multimode electromagnetically induced absorption transmission in metal-insulator-metal resonators

Cite as: AIP Advances **6**, 025219 (2016); https://doi.org/10.1063/1.4942937
Submitted: 29 October 2015 • Accepted: 16 February 2016 • Published Online: 23 February 2016

Dongdong Liu, Yue-Wu Pan, Yan Sun, et al.

Tunable multimode electromagnetically induced absorption transmission in metal-insulator-metal resonators

Dongdong Liu,[1,2] Yue-Wu Pan,[2] Yan Sun,[2] Xiushan Xia,[3] Jicheng Wang,[3,a] and Jian Lu[1,a]
[1]*School of Science, Nanjing University of Science & Technology, Nanjing 210094, China*
[2]*School of Mathematics & Physics Science, Xuzhou Institute of Technology, Xuzhou 221008, China*
[3]*School of Science, Jiangnan University, Wuxi 214122, China*

(Received 29 October 2015; accepted 16 February 2016; published online 23 February 2016)

The tunable multimode electromagnetically induced absorption (EIA)-like transmission was investigated in a two-ring system. In this system, by introducing asymmetry factor $\delta_i = \lambda_r - \lambda_{r'}$, we provided several ways to modulate the EIA-like transmission spectra. An off-to-on EIA-like response could be realized by changing the radius or the refractive index of the rings. During the off-to-on process, we found the red shift and blue shift effects in the spectra are appeared and the widths of EIA-like dips are broadened. Numerical simulation by finite element method was conducted to verify our discussion. We believe all these would provide guidelines to design the useful EIA-like devices. [http://dx.doi.org/10.1063/1.4942937]

I. INTRODUCTION

Surface plasmon polaritons (SPPs), which are the type of transverse electromagnetic waves, propagate along the interface between metal and dielectric material.[1] During last decades, SPPs have attracted tremendous attention for breaking the diffraction limitation.[2–4] Optical elements based on SPPs have been widely researched both in theory and experiment, such as filters,[5–7] modulators,[8] switches,[9–12] sensors[13–15] and so on. For instance, Wang *et al*[16] proposed a plasmonic filter based on a ring resonator. Chen *et al*[17] investigated a novel split-ring resonator with two metal-insulator-metal (MIM) waveguides.

Electromagnetically induced transparency (EIT), a quantum mechanical phenomenon, reduces light absorption over a narrow spectral region in a coherently driven atomic system.[18] Since the sharp resonance and steep dispersion could achieve in EIT, these systems show prominent potential for biosensor and optical data storage.[19] Recently, it has been demonstrated that EIT-like spectrum can be realized in classical configurations, such as the coupled dielectric resonators, the acoustic analogy of the EIT effect, the phase-coupled plasmonic induced transparency (PIT), and PIT in MIM waveguide bends.[20] However, electromagnetically induced absorption (EIA),[21] an opposite effect of EIT, results from atomic coherence induced by optical radiation, is less studied.

In this paper, we proposed a MIM structure composed of dual coupled ring resonators (DRRs) and two MIM waveguides. Numerical simulation by finite element method (FEM) was conducted to analyze our designs. The results showed EIA-like transmission in spectra. By changing the separation between rings, the radius or the refractive index of one ring, we would achieve an off-to-on EIA-like optical response. An asymmetry factor has been introduced to explain the corresponding transmission spectra. Based on the transmission characteristics, a tunable EIA-like device can be realized in our configuration.

[a]jcwang@jiangnan.edu.cn; lujian@mail.njust.edu.cn

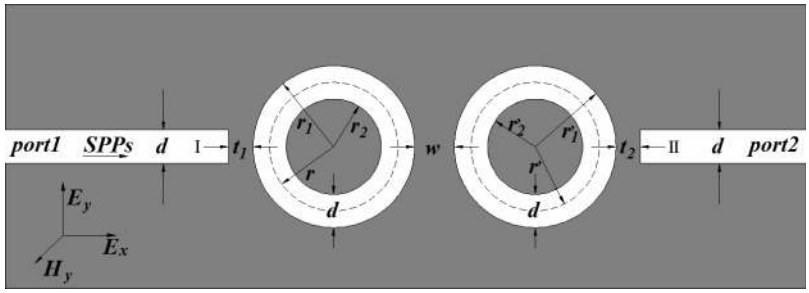

FIG. 1. Schematic of the structure composed of two ring resonators with two waveguides in shoulder arrangement. d is the width of the waveguides and the rings; r and r' are the radii of the left and the right ring resonator, respectively; t_1 and t_2 are the coupling distance between the waveguide and the ring, respectively; w is the coupling distance between the double rings.

II. MODEL AND THEORETICAL ANALYSIS

As shown schematically in Fig. 1, the plasmonic filter structure is composed of two ring resonators with two waveguides in shoulder arrangement. Port 1 and Port 2 are input and output ports, respectively. For simplicity, we assumed the media inside the rings and waveguides to be air. The widths of the waveguides and the rings are both d. The outer (inner) radii of the two rings are r_1 (r_2) and r_1' (r_2'), respectively. Meanwhile, we defined r=(r_1+r_2)/2 and r' = (r_1'+r_2') /2 as the radii of two ring resonators. t_1 and t_2 are the coupling distance between the waveguide and the ring, respectively. w is the coupling distance between the two rings. The metal is set as silver whose frequency-dependent dielectric constant is given by the well-known Drude model[22,23]:

$$\varepsilon_m(\omega) = \varepsilon_\infty - \frac{\omega_p^2}{\omega(\omega + i\gamma)}, \tag{1}$$

where ε_∞=3.7 is the dielectric constant at the infinite frequency, γ=2.73×10^{13}Hz is the electron collision frequency, ω_p=1.38×10^{16}Hz is the bulk plasma frequency and ω stands for the angular frequency of the incident electromagnetic radiation. In our discussion, the width d is chosen to be 50nm. Since d is much smaller than the incident wavelength λ, only the fundamental plasmonic mode TM_0 could exist in the waveguide. The propagation constant β of SPPs is determined by the following equation[24,25]:

$$\tanh\left(\frac{d\sqrt{\beta^2 - k_0^2\varepsilon_i}}{2}\right) = \frac{-\varepsilon_i\sqrt{\beta^2 - k_0^2\varepsilon_m(\omega)}}{\varepsilon_m(\omega)\sqrt{\beta^2 - k_0^2\varepsilon_i}}, \tag{2}$$

where ε_m and ε_i are the dielectric constants of the silver and air, respectively. k_0 is the wave vector of light in vacuum. The effective refractive index follows n_{eff}= β/k_0. It should be noted that the effective refractive index of the waveguides and ring resonators are assumed to be the same.[26] The real part of n_{eff} as a function of d and λ is shown in Fig. 2(a). For a fixed wavelength, Re (n_{eff}) gradually grows as wavelength λ increases.

III. SINGLE RESONATOR SYSTEM

At first, we discussed the single ring resonator system. The influence of some parameters on the transmission spectrum has been analyzed in the following. Theoretically, the resonant wavelength of the single ring resonator can be derived from the equation[16]:

$$\frac{J'_{n'}(kr_1)}{J'_{n'}(kr_2)} = \frac{N'_{n'}(kr_1)}{N'_{n'}(kr_2)}, \tag{3}$$

where $k = \omega(\varepsilon_0\varepsilon_\gamma\mu_0)^{1/2}$, ε_0 and μ_0 are the dielectric constant and permeability in vacuum, respectively. ε_γ=(n_{eff})^2/μ_0 is the frequency-dependent effective relative permittivity. $J_{n'}$ is the Bessel

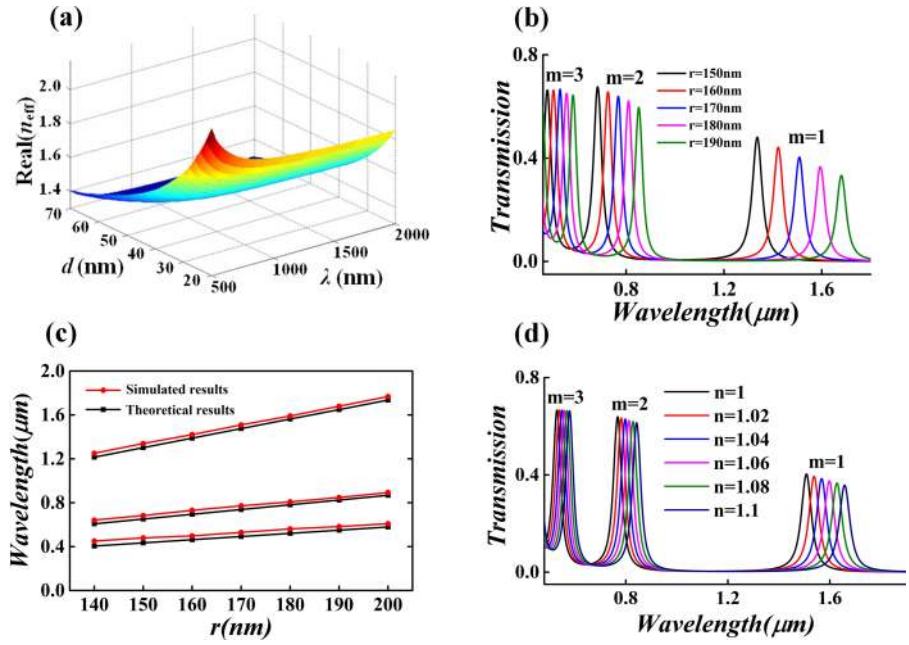

FIG. 2. (a) Real part of the effective refractive index n_{eff} versus the incident wavelength λ and the width d in MIM waveguide. (b) The transmission spectrum of the single ring resonator for different radius r with d=50nm, t=10nm and n=1. (c) The simulated and theoretical results of resonant wavelengths for different r. (d) The transmission spectra of the single ring resonator for different refractive index n with d=50nm, t=10nm and r=170nm.

function of the first kind with order n' and $N_{n'}$ is the Bessel function of the second kind with order n'. $J'_{n'}$ and $N'_{n'}$ are the derivatives of the Bessel functions to the argument kr. According to the reference,[23] we knew that the resonant wavelength also satisfies the simple relation $Re\ (n_{eff})\ L = m\lambda$, where m is resonant mode number, a positive integer.

Next, the effect of the radius r on transmission spectrum is studied. We set the radius r as from 150nm to 180nm at the step of 10nm, and set the other parameters as the same. The simulation results are depicted in Fig. 2(b). Apparently, as radius r grows, a red-shift is shown in the spectra and the transmission dips are becoming lower. And, the shifting effect is more obvious in low resonant modes. Moreover, we compared the simulated and theoretical results of resonant wavelengths for different r, shown in Fig. 2(c). The simulation results agree well with the theoretical results. Then, we researched the influence of refractive index n in the ring resonator. The refractive index n is changed from 1 to 1.1 at the step of 0.02 and other parameters are kept the same. The results were plotted in Fig. 2(d). As we can see, there is also a red-shift in spectra for a growing n. The red-shift is also more apparent in low resonant modes.

Furthermore, we plotted the field distributions at resonant modes and non-resonance mode, depicted in Fig. 3. We set n =1, d=50nm, r =170nm and t=10nm. As we know, when λ matches the resonant wavelength, SPPs form a standing wave inside the resonator and the energy could be well coupled to the output waveguide. This prediction has been well demonstrated in Fig. 3.

IV. DUAL COUPLED RING RESONATORS SYSTEM

In this section, we focused on a two-ring system, shown in Fig. 1. Further research revealed an EIA-like transmission spectrum in the two-ring system. We provided some approaches to tune the EIA-like transmission spectrum. At first, we discussed the influence of the coupling distance w. We set w as from 5nm to 25nm at the step of 5nm. Other geometric parameters were chosen as follows: $r = r'$ = 170nm, $t = t_1 = t_2$ =10nm and d = 50nm. The simulation results are plotted in Fig. 4. Compared with the transmission spectrum of the single-ring system, there are obvious EIA-like transmission dips in the spectra. As w decreases, the EIA-like dips at different modes are

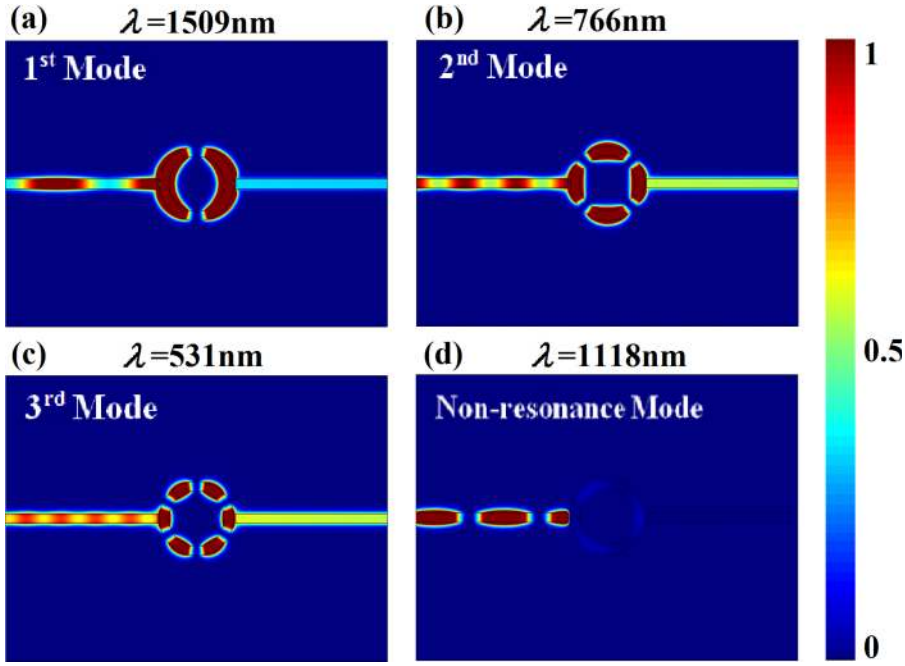

FIG. 3. The contour profiles of magnetic intensity distributions $|H_z|^2$ of the single ring resonator at different wavelengths with d=50nm, r=170nm, t=10nm and n=1 (a) λ=1509nm. (b) λ=766nm. (c) λ=531nm and (d) λ=1118nm.

becoming more apparent. This is because the interference between two resonators gets stronger when they are closer. Therefore, we found a way to achieve off-to-on response of EIA-like dips by varying the coupling distance w.

To get more insight into the physics of the EIA-like transmission spectra, the electric field distributions were visually illustrated in Fig. 5. The wavelengths are selected from the EIA-like dip region at different modes when w=5nm (Fig. 4). When the incident wavelength are λ=1550nm, 785nm and 542nm (the three new-born dips at 1st, 2nd, and 3rd mode), the two resonators interfere destructively with each other leading to EIA-like dips.

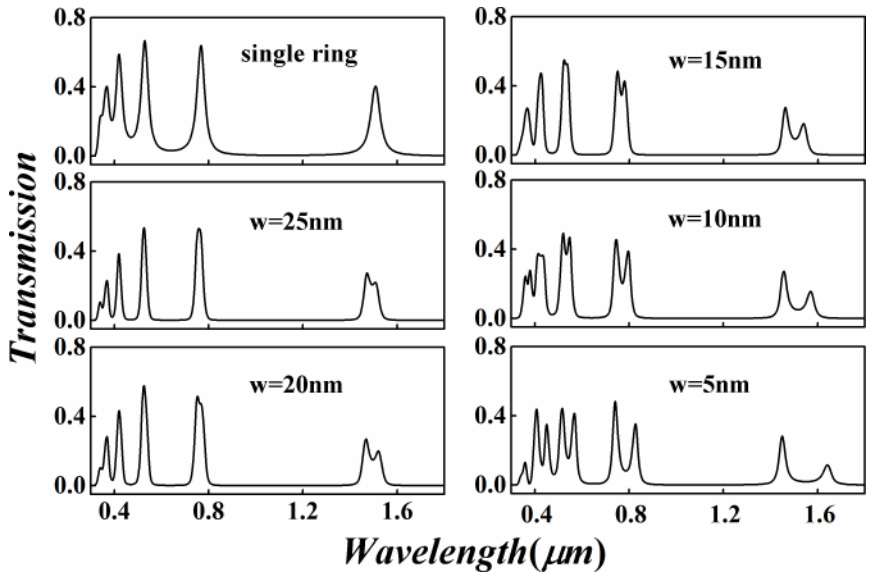

FIG. 4. Transmission spectra of single-ring and two-ring system with different separation w.

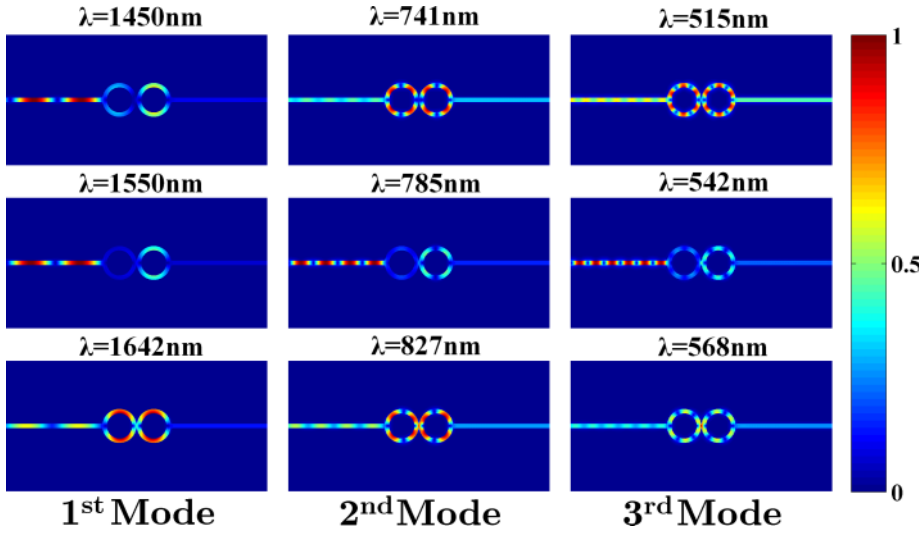

FIG. 5. Magnetic intensity distributions $|H_z|^2$ at the EIA-like dip region for 1st, 2nd and 3rd modes.

Next, we discussed the tunable EIA-like phenomena in the asymmetrical two-ring system. We defined the difference between resonant wavelengths of individual ring as asymmetry factor $\delta_i = \lambda_r - \lambda_{r'}$ (i=1, 2, 3 for each mode). The asymmetry factor can be controlled by varying the radii or the refractive index of the rings. In this part, we only changed the radius r' of the right ring from 150nm to 190nm at the step of 5nm, and set the left one as 170nm. The coupling distance t between the waveguide and the rings are chosen to be 10nm, and the separation w between two rings is set as 25nm. The simulation results are shown in Fig. 6. When r' ≥ 170nm, with a growing r', an obvious off-to-on multimode

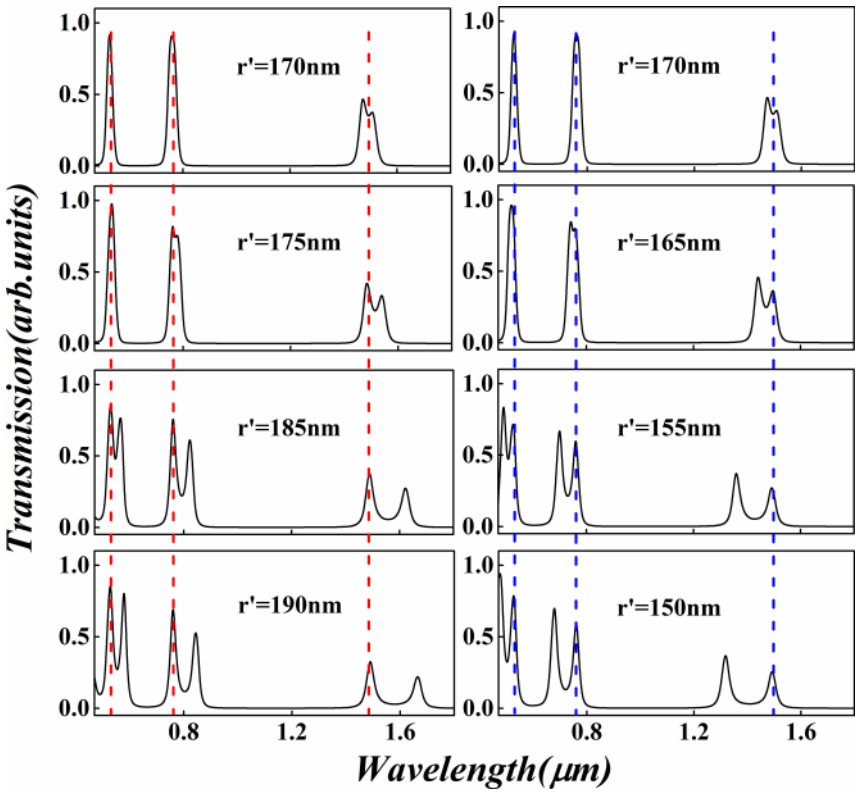

FIG. 6. Transmission spectra of two-ring system for different radius r'.

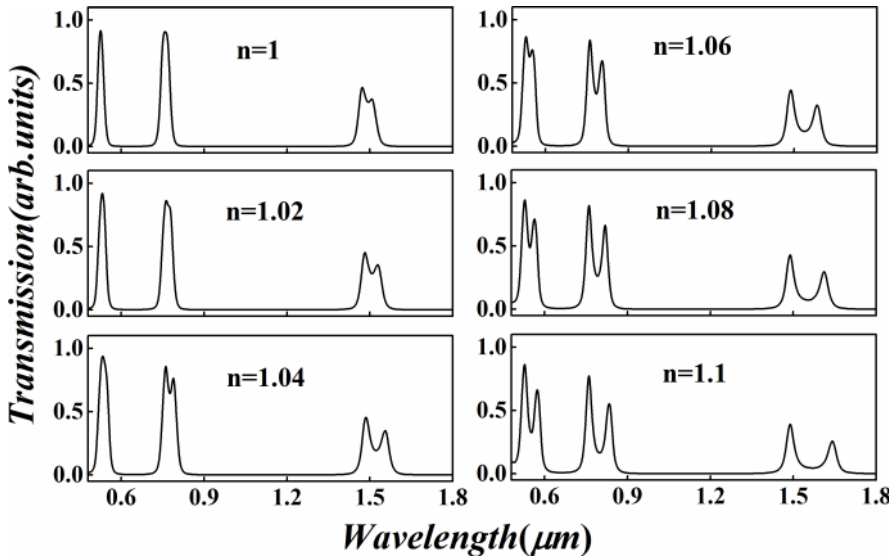

FIG. 7. Transmission spectra of two-ring system for different refractive index of the right ring.

EIA-like response can be observed, and the new-born absorption dips show a little red-shift. When $r' \leq 170$nm, with a decreasing r', the off-to-on multimode EIA-like response also appeared, but the new-born absorption dips show a little blue-shift. Interestingly, we found the shifting effect is more apparent and the width of absorption dips is wider at low resonant modes.

At last, we provided another way to introduce asymmetry factor by varying the refractive index of the right ring. The refractive index of the right ring was set as from 1 to 1.1 at the step of 0.02 and other parameters were kept the same as the above. We plotted the simulated results in Fig. 7. As n grows, the EIA-like dips are becoming more obvious and show a little red-shift in the spectra. Similarly, the shifting effect is more apparent and the width of absorption dips is wider at low resonant modes. From the aforesaid analysis, we found several guidelines to tune EIA-like transmission spectra in a two-ring system.

V. CONCLUSIONS

In summary, we studied the transmission characteristics of a structure composed of the MIM waveguides and ring resonators. At first, we discussed the influence of some parameters on the transmission spectrum in the single-ring system. We found both the radius and the refractive index of the ring can affect the resonant wavelength. Next, we discussed EIA-like transmission spectra in the two-ring system. By introducing asymmetry factor $\delta_i=\lambda_r - \lambda_{r'}$, we provided several approaches to tune the EIA-like transmission spectra. An off-to-on EIA-like response could be achieved by varying the radius or the refractive index of the rings. In addition, we found the shifting effect is more apparent and the width of absorption dips is wider at low resonant modes. All these analysis would provide guidelines to design an EIA-like device.

ACKNOWLEDGMENTS

This work is supported by the National Natural Science Foundation of China (Grant No. 11504139, 51172194, 11447149, 11347154), the Natural Science Foundation of Jiangsu Province (Grant No. BK20140167), and the Nature Science Foundation of Xuzhou Institute of Technology (Grand No.XKY2014206, XKY2014308).

[1] W. L. Barnes, A. Dereux, and T. W Ebbesen, "Surface plasmon subwavelength optics," Nature **424**, 824 (2003).
[2] C. Genet and T. W. Ebbesen, "Light in tiny holes," Nature **445**, 39 (2007).

[3] P. Neutens, P. Van Dorpe, I. De Vlaminck, L. Lagae, and G. Borghs, "Electrical detection of confined gap plasmons in metal-insulator-metal waveguides," Nat. photon. **3**, 283 (2009).
[4] D. K. Gramotnev and S. I. Bozhevolnyi, "Plasmonics beyond the diffraction limit," Nat. photon. **4**, 83 (2010).
[5] I. Zand, M. Bahramipanah, M. S. Abrishamian, and J. M. Liu, "Metal-insulator-metal nanoscale loop-stub structures," IEEE Photon. J **4**, 2136 (2012).
[6] H. Lu, X. M. Liu, D. Mao, L.R. Wang, and Y. K. Gong, "Tunable band-pass plasmonic waveguide filters with nanodisk resonators," Opt. Express **18**, 17922 (2010).
[7] H. Lu, X. M. Liu, Y.K. Gong, L. R. Wang, and D. Mao, "Multi-channel plasmonic waveguide filters with disk-shaped nanocavities," Opt. Commun. **284**, 2613 (2011).
[8] W. Cai, J.S. White, and M.L. Brongersma, "Compact, high-speed and power-efficient electro-optic plasmonic modulators," Nano Lett. **9**, 4403 (2009).
[9] C. Janke, J. G. Rivas, P. H. Bolivar, and H. Kurz, "All-optical switching of the transmission of electromagnetic radiation through subwavelength apertures," Opt. Lett. **30**, 2357 (2005).
[10] C. J. Min, P. Wang, C. C. Chen, Y. Deng, Y. H. Lu, H. Ming, T. Y. Ning, Y. L. Zhou, and G. Z. Yang, "All optical switching in subwavelength metallic grating structure containing nonlinear optical materials," Opt. Lett. **33**, 869 (2008).
[11] G. A. Wurtz, R. Pollard, and A. V. Zayats, "Optical bistability in nonlinear surface-plasmon polaritonic crystals," Phys. Rev. Lett. **97**, 057402 (2010).
[12] M. Sluijter, D. K.G. de Boer, and H. P. Urbach, "Simulations of a liquid-crystal-based electro-optical switch," Opt. Lett. **34**, 94 (2008).
[13] B. Gallinet and O. J. F. Martin, "Refractive index sensing with subradiant modes: A framework to reduce losses in plasmonic nanostructures," ACS Nano. **7**, 6978 (2013).
[14] V. E. Bochenkov, M. Frederiksen, and D. S. Sutherland, "Enhanced refractive index sensitivity of elevated short range ordered nanohole arrays in optically thin plasmonic Au films," Opt. Express **21**, 14763 (2013).
[15] T. S. Wu, Y. M. Liu, Z. Y. Yu, Y. W. Peng, C. G. Shu, and H. Ye, "The sensing characteristics of plasmonic waveguide with a ring resonator," Opt. Express **22**, 7669 (2014).
[16] T. B. Wang, X. W. Wen, C. P. Yin, and H. Z. Wang, "The transmission characteristics of surface plasmon polaritons in ring resonator," Opt. Express **17**, 24096 (2009).
[17] J. Chen, Y. D. Li, Z. Q. Chen, J. Y. Peng, J. Qian, J. J. Xu, and Q. Sun, "Tunable resonances in the plasmonic split-ring resonator," IEEE Photon. J. **6**, 1 (2014).
[18] Z. Zhang, L. Zhang, H. Li, and H. Chen, "Plasmon induced transparency in a surface Plasmon polariton waveguide with a comb line slot and rectangle cavity," Appl. Phys. Lett. **104**, 231114 (2014).
[19] R. D. Kekatpure, E. S. Barnard, W. Cai, and M. L. Brongersma, "Phase-coupled plasmon-induced transparency," Phys. Rev. Lett. **104**, 243902 (2010).
[20] Z. H. He, H. J. Li, S. P. Zhan, G. T. Cao, and B. X. Li, "Combined theoretical analysis for plasmon-induced transparency in waveguide systems," Opt. Lett. **39**, 5543 (2014).
[21] A. Lezama, S. Barreiro, and A. M. Akulshin, "Electromagnetically induced absorption," Phys. Rev. A. **59**, 4732 (1999).
[22] A. D. Rakic, A. B. Djurišic, J. M. Elazar, and M. L. Majewski, "Optical properties of metallic films for vertical-cavityoptoelectronic devices," Appl. Opt. **37**, 5271 (1998).
[23] Z. Han and S. I. Bozhevolnyi, "Plasmon-induced transparency with detuned ultracompact Fabry-Perot resonators in integrated plasmonic devices," Opt. Exp. **19**, 3251 (2011).
[24] B. Tang, J. Wang, X. Xia, X. Liang, C. Song, and S. Qu, "Plasmonic induced transparency and unidirectional control based on the waveguide structure with quadrant ring resonators," Appl. Phys. Exp. **8**, 032202 (2015).
[25] F. Lu, Z. Wang, K. Li, and A. Xu, "A plasmonic triple-wavelength demultiplexing structure based on MIM waveguide with side-coupled nanodisk cavities," IEEE Trans. Nanotechnol. **12**, 1185 (2013).
[26] G. G. Zheng, W. Su, Y. Y. Chen, C.Y. Zhang, M. Lai, and Y. Z. Liu, "Band-stop filters based on a coupled circular ring metal–insulator–metal resonator containing nonlinear material," J. Opt. **14**, 055001 (2012).